

1 Supplementary Materials for

2

3 **Azacytidine targeting SARS-CoV-2 viral RNA as a potential**
4 **treatment for COVID-19**

5

6 **This Supplementary file includes:**

7

8 Materials and Methods

9 Figures. S1 to S13, and Supplementary Table 1

10

11 **Materials and Methods**

12 ***Cells, virus, and reagents***

13 Vero E6 cells were obtained from the American Type Culture Collection
14 (ATCC-1586) and cultured in Dulbecco's modified Eagle's medium (DMEM;
15 Gibco), supplemented with 10% fetal bovine serum (FBS; Gibco), penicillin (100
16 U/ml), and streptomycin (100 µg/ml), at 37°C in a humidified 5% CO₂ incubator.

17 SARS-CoV-2 (nCoV-2019BetaCoV/Wuhan/WIV04/2019) was propagated
18 in Vero E6 cells. Viral titer was determined through plaque assay. Prof. Meilin
19 Jin from Huazhong Agricultural University provided mouse-adaptive SARS-
20 CoV-2 (MA-SARS-CoV-2), which was created through continuously passaging
21 wild virus in aged mouse lungs^[1]. All infection experiments were performed in
22 a biosafety level-3 (BSL-3) laboratory.

23 5-Azacytidine (5Aza), Remdesivir (RDV), and Chloroquine (CQ) were
24 obtained from MedChemExpress and dissolved in sterile saline and water,
25 respectively.

26 Lipo8000 (Beyotime Biotechnology, China) was used to transfect plasmids
27 and siRNA according to the instruction.

28 ***Evaluation of cytotoxicity***

29 Vero E6 cells were incubated with different 5Aza concentrations in 96-well
30 plates for 24h. Cytotoxicity was measured using CCK-8 assay. CC₅₀ was
31 calculated in Prism (GraphPad).

32 ***Quantitative reverse transcription-PCR (qRT-PCR)***

33 Viral RNA was extracted using the TaKaRa MiniBEST Viral RNA/DNA
34 Extraction Kit (Cat No. 9766). RNA was eluted in 40 µl RNase-free water. Viral
35 RNA copy number was determined with TaqMan-based qRT-PCR using the
36 One Step PrimeScript RT-PCR Kit (Takara, RR064A). To generate a standard
37 curve, the receptor binding domain (RBD) of the spike gene was amplified and
38 its copy number determined from serial dilutions. Primers used for qRT-PCR
39 were RBD-F: CAATGGTTTAAACAGGCACAGG, RBD-R:

40 CTCAAGTGTCTGTGGATCACG, and RBD-probe: 5'-FAM-
41 ACAGCATCAGTAGTGTCAGCAATGTCTC-BHQ 3'. The thermocycling
42 schedule was as follows: 95°C for 2 min, followed by 40 cycles of 95°C for 5 s
43 and 60°C for 30 s. The half-maximal inhibitory concentration (IC₅₀) of 5Aza was
44 calculated in GraphPad.

45 ***Immunofluorescence microscopy***

46 Cells were fixed overnight with 4% paraformaldehyde, permeabilized with
47 0.05% Triton X-10 for 10 min, and blocked with 5% bovine serum albumin (BSA)
48 for 1 h. They were then incubated for 2 h at room temperature with a primary
49 antibody against viral N protein (1:500 dilution, Sino Biological), followed by
50 incubation with Alexa 488-labeled goat anti-rabbit IgG (1:500 dilution,
51 Proteintech) for 1 h. Nuclei were stained with DAPI (Beyotime Biotechnology).
52 Images were captured with fluorescence microscopy.

53 ***Plaque assay***

54 Vero E6 cells (~1 × 10⁵ cells) were incubated in DMEM containing SARS-
55 CoV-2. After 1 h, the supernatant was removed and the cells were incubated in
56 an overlay medium containing DMEM with 2% FBS and 0.9% CMC
57 (Calbiochem). After 96 h, the cells were fixed overnight using 4%
58 paraformaldehyde and stained with crystal violet.

59 ***Time-of-drug-addition assay***

60 A time-of-drug-addition assay was performed to determine the SARS-CoV-
61 2 life-cycle stage that 5Aza affects. For "Entry," Vero E6 cells were pretreated
62 with 24 μM 5Aza for 1 h and infected with 0.01 MOI SARS-CoV-2. Two hours
63 (h) later, the cells were washed twice with DMEM and placed in fresh culture
64 medium. For "Post-entry," the cells were infected with virus for 2 h, then washed
65 twice and cultured with fresh medium containing 24 μM 5Aza. For "Full-time,"
66 cells were pretreated with 24 μM 5Aza for 1 h and infected with SARS-CoV-2
67 for 2 h. Subsequently, the cells were washed twice and cultured with fresh
68 medium containing 24 μM 5Aza until the experiment ended. After 24 and 48

69 hours, supernatants were collected, cells were fixed, and total proteins were
70 extracted for qRT-PCR, fluorescence microscopy, and western blotting,
71 respectively.

72 ***RNA immunoprecipitation***

73 Vero E6 cells seed in 10-cm plate were transfected with pCAGGS/HA
74 expressing eGFP, DNMT2, or NSUN2. 24 hours later, cells were infected with
75 0.2 SARS-CoV-2 for 20 hours in the presence of 16 μ M 5Aza or not. Cells were
76 lysed with RIP lysis buffer (gzscbio, Guangzhou, China) with inhibitor cocktail.
77 1% of the lysates was collected for input analysis, and 3% of lysates were
78 collected for WB analysis. RNAs of remaining lysates were immunoprecipitated
79 by anti-HA agarose in the presence of RNase inhibitor and 0.2 M EDTA at 4°C
80 overnight. After washing with RIP buffer for 8 times, 20% of the agarose was
81 denatured for IPed protein detection, the remaining was subjected to 10% SDS
82 and proteinase K treatment at 65°C for 45 min. Then the supernatant was
83 collected for RNA extraction, followed by RT-PCR for SARS-CoV-2 RNA
84 detection.

85 ***Western blotting***

86 Cells were lysed with RIPA buffer (Thermo, 89900) containing a protease
87 inhibitor cocktail (MCE). Proteins were separated using 10% SDS-PAGE and
88 then transferred onto PVDF membranes (Millipore). Membranes were blocked
89 in Tris Buffered Saline (TBS) buffer with 0.1% Tween-20 (TBST) for 1 h at room
90 temperature, followed by incubation with a primary antibody against viral N
91 protein for 2 h at room temperature. After washing with TBST three times, the
92 membranes were incubated with a secondary peroxidase-conjugated antibody
93 (1:5000 dilution, Proteintech). GAPDH was used as the internal control. Bands
94 were detected using WesternBright ECL (Advansta).

95 ***Animal experiments***

96 Female BALB/c mice (8 weeks old) were obtained from Snac Jinda
97 Laboratory Science (Hunan Province, China) and randomly divided into five

98 groups (Control, 5Aza, Control + SARS-CoV-2, 5Aza + SARS-CoV-2, and
99 Remdesivir + SARS-CoV-2; n = 10 per group). On Day 0, mice were
100 anesthetized using isoflurane. Infection groups were intranasally challenged
101 with 4×10^3 PFU MA-SARS-CoV-2 in 50 μ l DMEM, while the un-infection
102 groups were treated with 50 μ l DMEM only. One day later, mice were
103 intraperitoneally injected with 2 mg/kg 5Aza (Control and 5Aza + SARS-CoV-2
104 groups), 25 mg/kg Remdesivir (Remdesivir + SARS-CoV-2 group) or an
105 equivalent volume of sterile saline (Control and Control + SARS-CoV-2 groups),
106 once daily for seven consecutive doses. Body weight was measured daily for
107 14 d; mouse with more than 30% of body weight loss was immediately
108 euthanized and regarded to be dead, and mouse survival rates were calculated
109 (n = 6). At 4 dpi, four mice from each group were euthanized for lung collecting.
110 Tissues were used for the qRT-PCR quantification of viral RNA copy number
111 and H&E staining for histopathological changes.

112 All animals were bred in a specific pathogen-free animal facility;
113 experiments were performed in a biosafety level-3 (BSL-3) laboratory and were
114 approved by the Institutional Animal Care and Use Committee of Wuhan
115 Institution of Virology, CAS (No. WIVA04202004).

116 ***Bisulfite library preparation, RNA library preparation, and next-generation*** 117 ***sequencing***

118 Total RNA (200 ng) was treated with the MGIEasy rRNA Depletion Kit for
119 rRNA removal, bisulfite-converted using the EZ RNA Methylation Kit (Zymo
120 Research), and then fractionated into long and small RNA fractions.

121 The transcriptome library of bisulfate RNA or non-bisulfate RNA was
122 constructed using the MGIEasy RNA Directional Library Prep Kit (without ligase
123 in the second strand synthesis). Samples were sequenced using the PE100+10
124 bp method. ERCC was used as negative control and helped to correct false
125 positive sites. The ERCC without any methylation could be used to assay the
126 RNA bisulfite conversation rate.

127 ***Nanopore direct RNA sequencing***

128 Total RNA (1 µg) was treated with the MGIEasy rRNA Depletion Kit to
129 remove rRNA. Next, a direct RNA Sequencing kit (SQKRNA002) was
130 used to prepare RNA with 1D sequencing on an Oxford Nanopore
131 equipment. Data were analyzed using an established pipeline.

132 ***Quality control***

133 Firstly, a custom Python script was used to demultiplex the barcode list.
134 Secondly, adapter trimming and quality pruning were analyzed with fastp.
135 Bases in the sliding window with mean quality below 20 were cut, and raw reads
136 of those containing 5 or 3 bp adapters were trimmed. mRNA was trimmed to
137 nine bp from the left end.

138 ***Mapping and calling***

139 C2T and G2A reference genomes were converted for building indexes
140 using bismark _genome_preparation. Clean sequencing reads were aligned to
141 the two reference genomes with Bismark. Methylation calls were stored in BAM
142 files generated during this step. BAM files were used to ensure that reads were
143 mapped to the same direction and had the same start positions, mapping length,
144 and molecular tag. Bismark_methylation_extractor was used to obtain readable
145 results for downstream analysis.

146 ***Quantity and differential expression***

147 Transcript quantification was performed using HTSeq v0.44.0. RNA with
148 zero counts in all samples was removed. Normalization and differential
149 expression were determined using the R package DEseq2 v1.28.1.

150 ***Differentially methylated regions***

151 After alignment, we extracted methylation counts from Bismark output; then,
152 DMRfinder was used to cluster CpG sites into test regions for differential
153 methylation.

154 ***Sample preparation for nucleotide modification***

155 For DNA and RNA extraction, cells were lysed with TRIzol reagent and
156 digested with proteinase K at 37°C for 30 min. An equal volume of back
157 extraction buffer (4 M guanidine thiocyanate, 50 mM sodium citrate, 1 M Tris,
158 pH 8.0) and 1/10 volume of 3 M sodium acetate (pH 4.0) was mixed with the
159 cell lysate. Samples were then centrifuged at 13,200 rpm for 15 min at 4°C. The
160 upper phase was transferred to a new tube and an equal volume of 100%
161 isopropanol was added. After overnight incubation at -80°C, samples were
162 centrifuged at 13,200 rpm and 4°C for 15 min. The supernatant was removed
163 and pellets were washed twice with 70% ethanol. Samples were eluted with 50
164 µl nuclease-free buffer and centrifuged at 5,000 rpm for 2 min. The supernatant
165 was then transferred to a new tube. Total RNA was extracted using TRIzol
166 reagent. RNA or DNA/RNA hybrid (500 ng) was digested into nucleotides using
167 20 µl Nucleoside Digestion Mix (NEB, M0649S). The digestion product was
168 brought to 50 µl with nuclease-free water and filtered using a Microcon-10kDa
169 Centrifugal Filter Unit with Ultracel-10 membrane.

170 ***LC-MS/MS***

171 The analysis used an ACQUITY UPLC I-Class system coupled with a
172 QTRAP 6500+ triple quadrupole mass spectrometer (Sciex, Framingham, MA).
173 Nucleotide samples were diluted five times, and 10 µl of each dilution was
174 chromatographed on HSS T3 C18 (100 x 2.1 mm, 1.8 µm, Waters, Milford, MA).
175 Samples were eluted with a linear gradient of A (0.2% formic acid + 5 mM
176 ammonium formate in deionized water) and B (0.2% formic acid + 5 mM
177 ammonium formate in methanol) at a flow rate of 0.3 ml/min and temperature
178 of 45°C. The gradient elution started with 96% of mobile phase A for 2.5 min.
179 Next, mobile phase B was linearly increased up to 45% in 2.5 min and
180 maintained for 0.5 min, then linearly increased up to 100% in 2 min. Finally, the
181 combination was brought back to 96% A in 1 min. Detection was achieved using
182 a QTRAP 6500+ system in positive ion mode and multiple reaction monitoring
183 mode (MRM). Source parameters were set as follows: temperature, 400°C;

184 curtain gas (CUR), 30; collision gas, low; ion spray voltage, 5000 V; ion source
185 gas (GS1), 45; and drying gas (GS2), 40.

186 ***Statistical analysis***

187 Statistical significance was determined by Student's *t* test for two groups.

188 Analysis with a probability value < 0.05 were considered statistically significant.

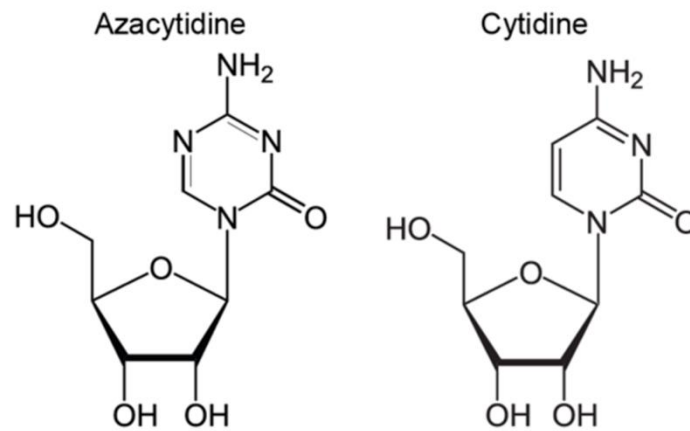
189

190 **Reference**

191 [1] Huang K, Zhang Y, Hui X, et al. Q493k and q498h substitutions in spike
192 promote adaptation of sars-cov-2 in mice. *EBioMedicine*, 67 (2021), p. 103381

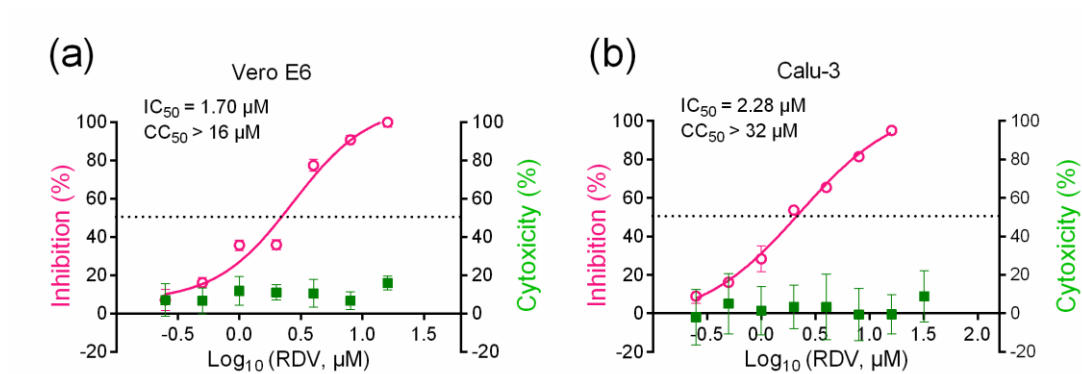
193

194 **Supplementary figures**



195 **Fig.S1 Molecular structures of cytidine and azacytidine.**

196

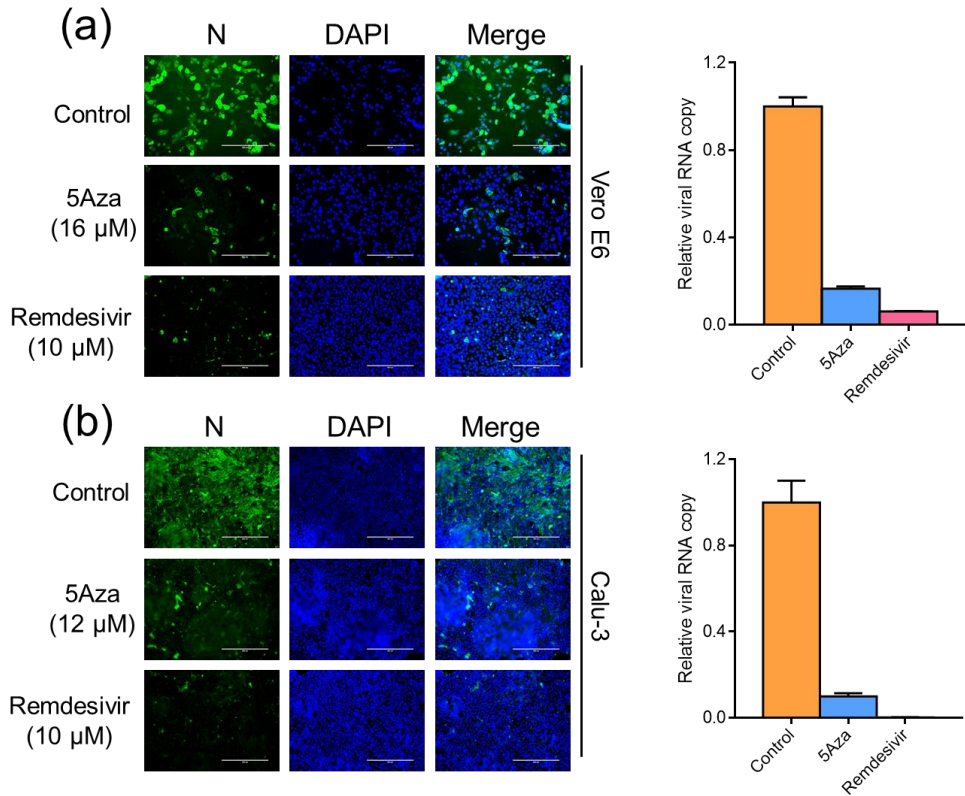


197

198 **Fig.S2 Remdesivir inhibits SARS-CoV-2 in Vero E6 and Calu-3 cells**

199 Vero E6 (a) and Calu-3 (b) cells were infected with 0.2 moi SARS-CoV-2, in the
200 presence of various concentration of Remdesivir (RDV). After 24 hpi,
201 supernatant was collected. IC₅₀ was calculated by detecting viral RNA copies
202 through qRT-PCR. And cytotoxicity of RDV was determined through CCK-8
203 assay. Left and right Y-axes represent mean % inhibition of virus and %
204 cytotoxicity of 5Aza, respectively.

205

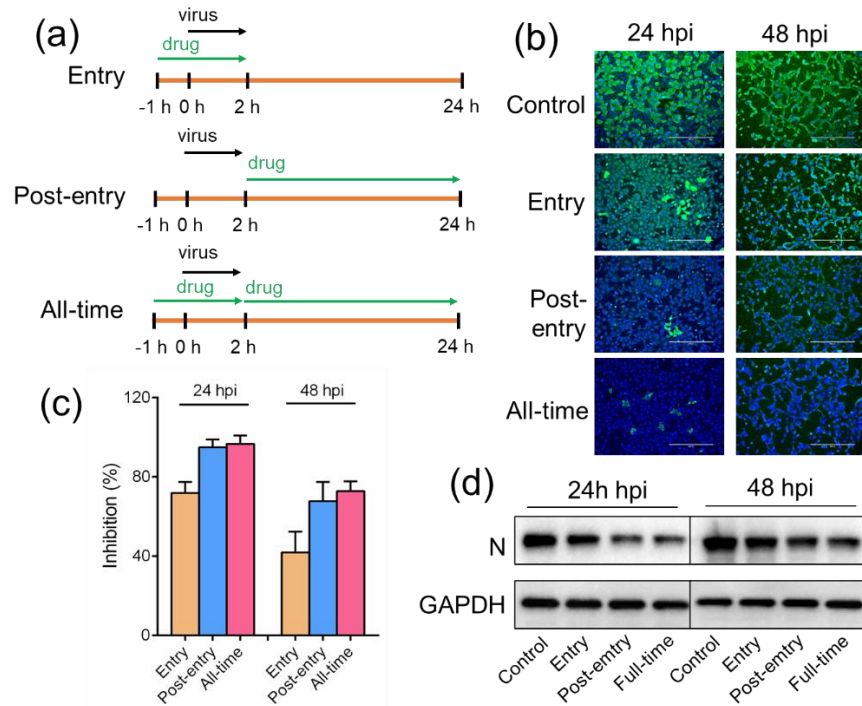


206

207 **Fig.S3 Indirect immunofluorescence detecting of SARS-CoV-2.**

208 Vero (a) and Calu-3 (b) were infected with 0.2 moi SARS-CoV-2 in the presence
 209 of indicated drugs. Twenty-four hours later, the supernatant was collected for
 210 RNA detection; cells were fixed by 4% paraformaldehyde for
 211 immunofluorescence assay of viral N protein. Nuclei were stained with DAPI.
 212 Bars, 200 μ M. All experiments were performed in triplicate; data are mean \pm
 213 SD.

214



215

216 **Fig.S4 Time-of-drug-addition experiment of 5Aza.**

217 (a) Schematic of time-of-drug-function experiment of 5Aza. Vero E6 cells were

218 treated with 5Aza and then infected with 0.01 moi SARS-CoV-2. (b) After 24

219 and 48 hpi, supernatant was collected for detecting RNA copies using qRT-

220 PCR. (c) cells were fixed for immunofluorescence assay of viral N protein, and

221 (d) total proteins were extracted for western blotting to detect N protein. Nuclei

222 were stained with DAPI. Bars, 200 μ M. Data are mean \pm SD.

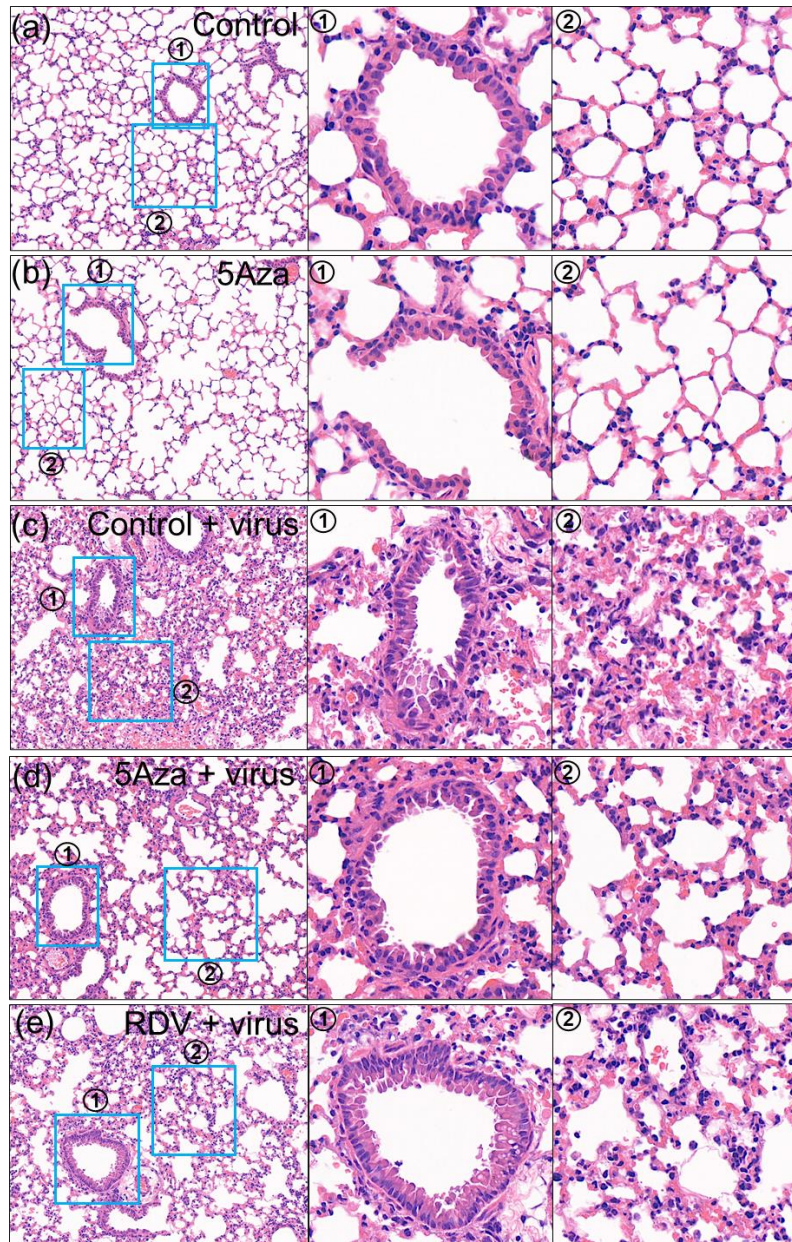
223

224

225

226

227

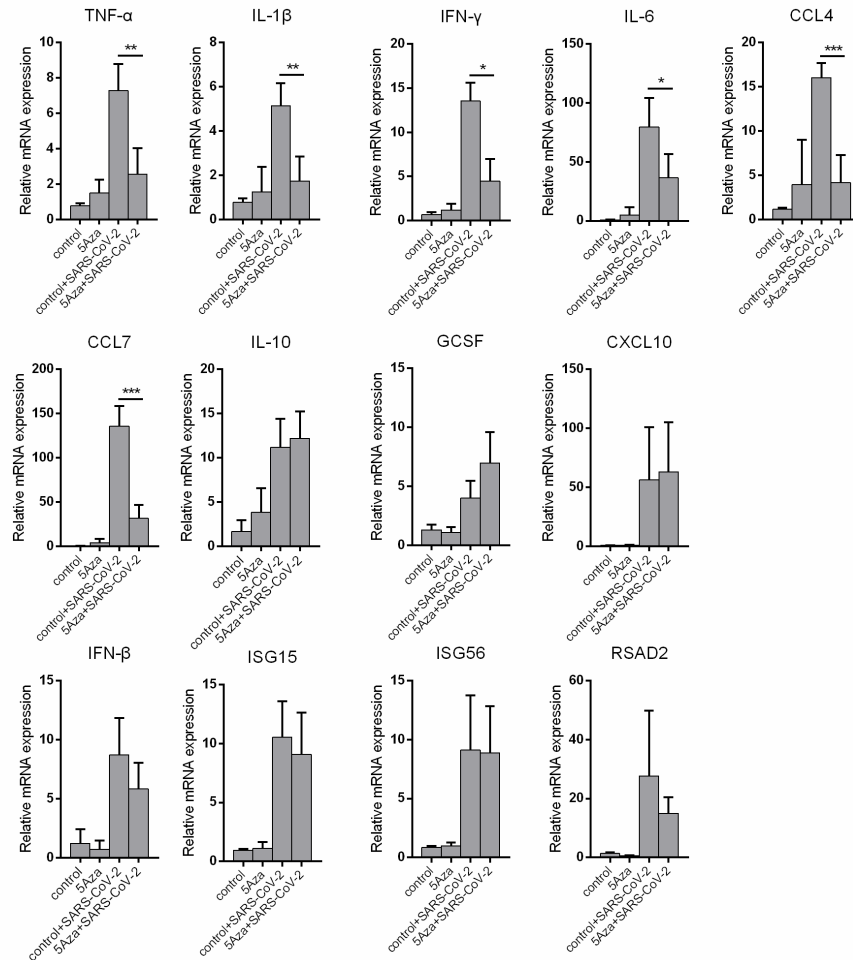


228

229 **Fig.S5 H&E staining of lung tissues.**

230 At 4 dpi, mice were euthanized, and lungs were collected for histopathological
 231 analysis with H&E staining. Numbered blue rectangles are shown in magnified
 232 images to the right. (a) and (b) Lung tissues were normal in the mock infection
 233 group. (c) Lung tissue section from the control + SARS-CoV-2 group mice
 234 displayed (1) bronchiolar epithelium cell death, (2) destruction of alveola with
 235 massive infiltration. (d) and (e) Representative image of lung tissue from 5Aza
 236 and Remdesivir treated infection group mice showing alleviated infiltration.

237



238

239 **Fig.S6 The cytokines expression in lungs.**

240 Total RNA of lungs was extracted using Trizol. 1 μg RNA was inversely

241 transcribed for detection of indicated genes by qRT-PCR. Gene expression was

242 normalized to that of GAPDH. Data are mean ± SD, and analyzed using

243 Student's *t* test. * $p < 0.05$, ** $p < 0.01$, *** $p < 0.001$.

244

245

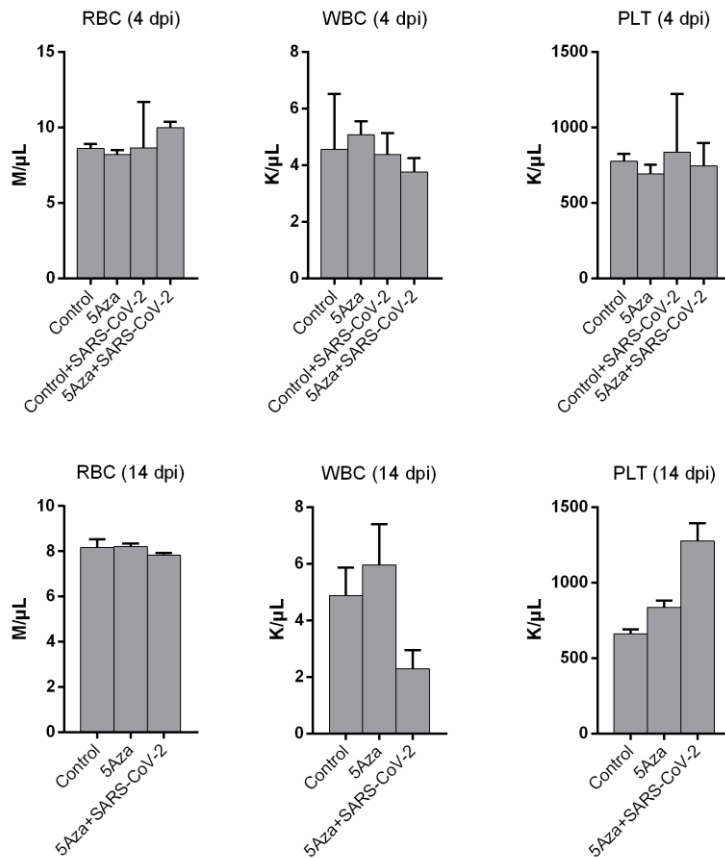
246

247

248

249

250



251

252 **Fig.S7 Detection of RBC, WBC, and PLT in mice blood.**

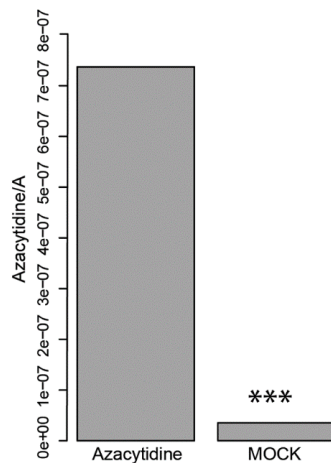
253 Whole blood from four mice at indicated days was collected with anticoagulation.

254 And Red blood cell (RBC), White blood cell (WBC), and blood platelet (PLT)

255 were determined. At 14 dpi, none mouse survived in Control + SARS-CoV-2

256 group, and therefore this data is absence.

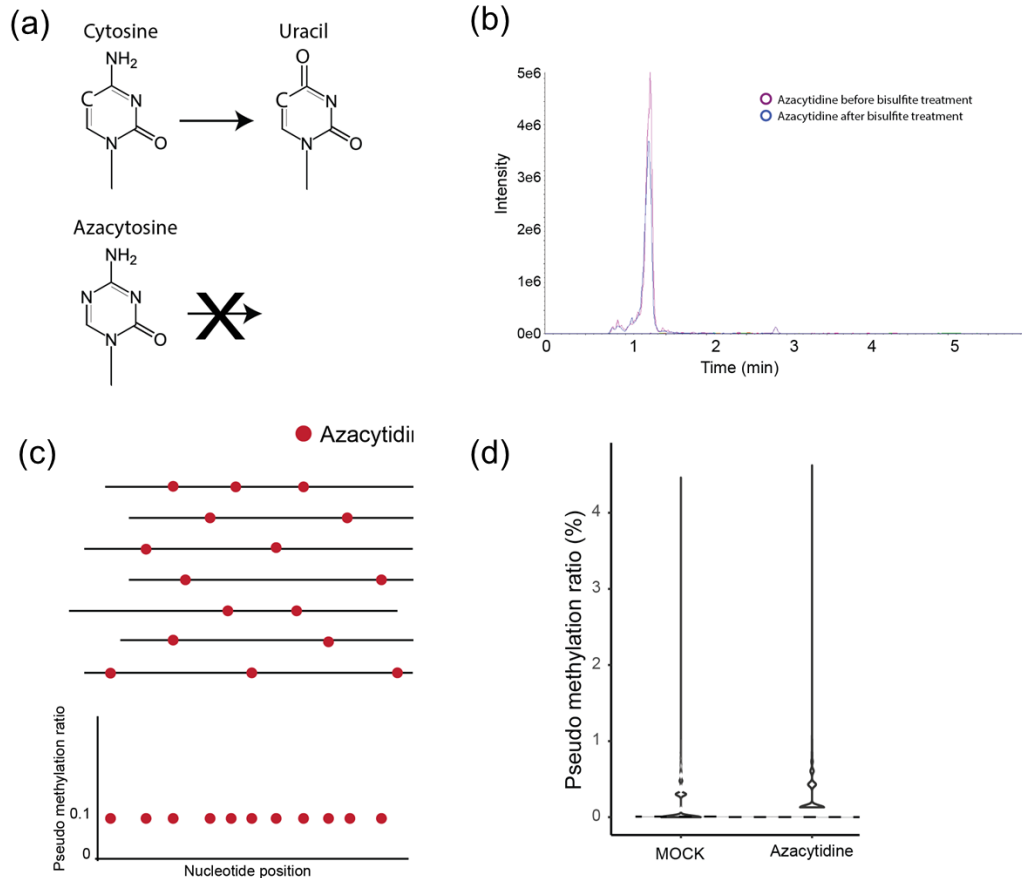
257



258

259 **Fig.S8 Profiling and quantification of azacytidine in DNA and RNA using**
260 **liquid chromatography-tandem mass spectrometry (LC-MS/MS).**

261 Considering azacytidine as an RNA analog with OH-group on ribose 2' carbon
262 (2' C), it could theoretically incorporate into RNAs. "Azacytidine" sample were
263 the cells incubated with 5Aza (10 μ M) for 24 h and "Mock" sample were the
264 cells without any treatment. Both DNA and RNA were extracted, followed by
265 single nucleotide digestion (DNA and RNA) and LC-MS/MS. Azacytidine was
266 normalized to adenosine on the y-axis. Data are presented as means of
267 triplicate assays ($***p < 0.001$). Most of the azacytidine incorporated into the
268 RNAs. This was consistent with previous reports, in which radiolabelled
269 azacytidine was measured by scintillation-based quantification or high-
270 resolution mass spectrum termed "AZA-MS".



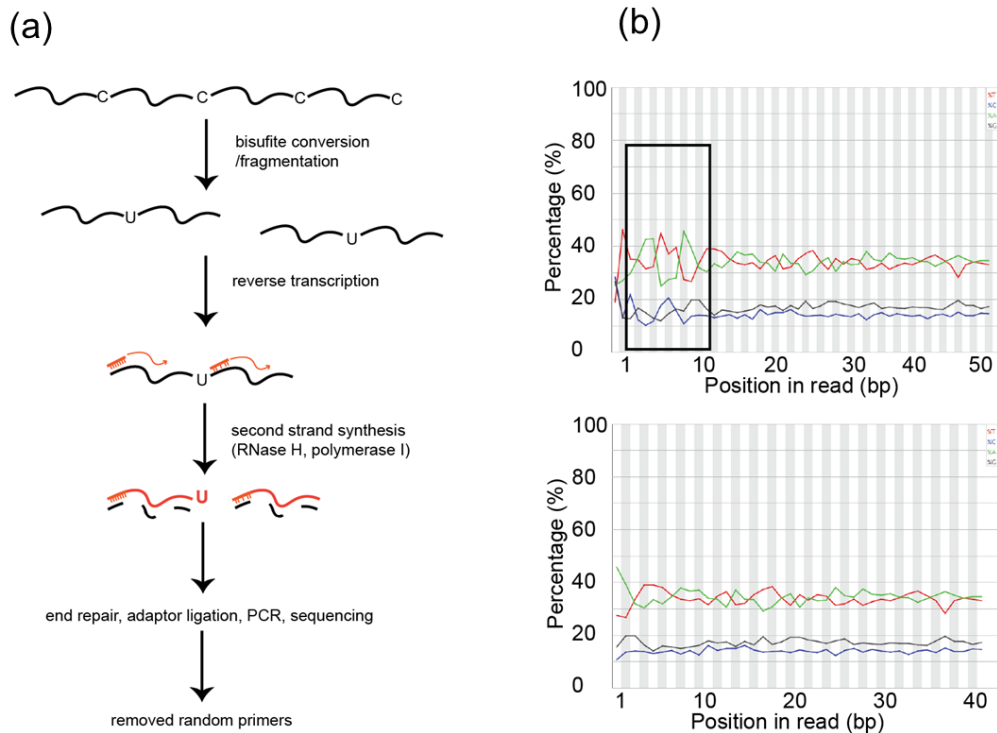
271

272 **Fig.S9 5Aza-BSseq-identified locations of 5Aza incorporation.**

273 (a) We explored whether azacytidine could be converted to uracil under
 274 bisulfite treatment and found that was not the case. Bisulfite deamination of
 275 cytidine relies on Lewis acid formation and electron transfer from C5. In
 276 azacytidine, N5 inhibited this deamination. (b) LC-MS chromatograms of 5Aza
 277 before and after bisulfite treatment. Supporting the observation in (a), LC-MS
 278 chromatograms of azacytidine remained unchanged before and after bisulfite
 279 treatment. (c) Schematic diagram of testing pseudo-methylation sites. This
 280 chemical property of azacytidine is similar to the RNA m⁵C, which also cannot
 281 be converted to uracil in bisulfite sequencing. Unconverted azacytidine may be
 282 identified as a pseudo cytidine (pseudo-methylation) site in RNA bisulfite
 283 sequencing. Owing to randomized azacytidine incorporation, these azacytidine
 284 (pseudo-methylation) sites should be observed as increased ultra-low
 285 methylation (methylation ratio <1%). (d) The ratio of pseudo-methylation.

286 Pseudo-methylation distribution analysis revealed that azacytidine treatment
 287 increased ultra-low pseudo-methylation (<1%), indicating 5Aza incorporation in
 288 RNA.

289

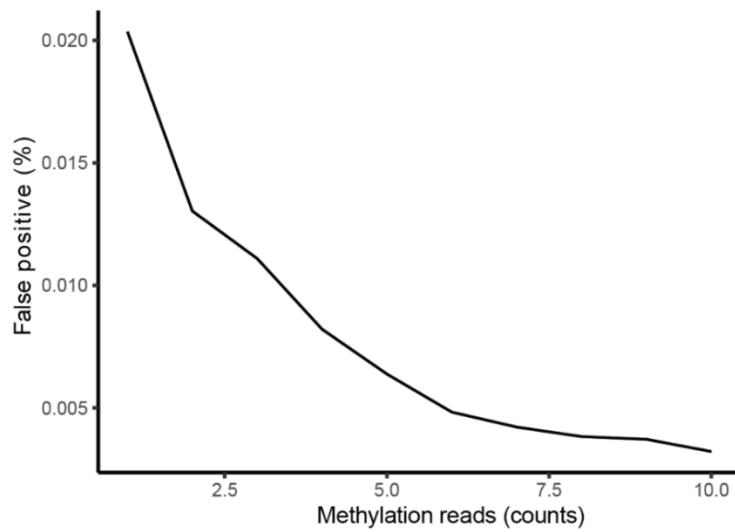


290

291 **Fig.S10 Experimental flowchart of RNA-BSseq.**

292 Limitations in site-mapping technology hamper the validity of coronavirus RNA
 293 methylation. As random priming in RNA bisulfite sequencing introduces
 294 mismatch errors, it is difficult to reliably measure m⁵C sites. We sought to
 295 develop an optimized approach that avoids random primer insertion into
 296 sequenced fragments, thus minimizing false positives. (a) Without using ligase
 297 in second strand synthesis, we could remove random primers in the middle of
 298 sequenced fragments. During bioinformatics analysis, we could then easily
 299 detect and delete the first six bases affected by random primers initializing
 300 reverse transcription. (b) Nucleotide density distribution (A, T, C, or G) in
 301 sequencing reads. Upper and lower panels show distribution before and after
 302 the removal of random primer sequences, respectively. The distribution

303 fluctuated before and after a smooth line, indicating a few artifact Cs in our
304 modified bisulfite sequencing.



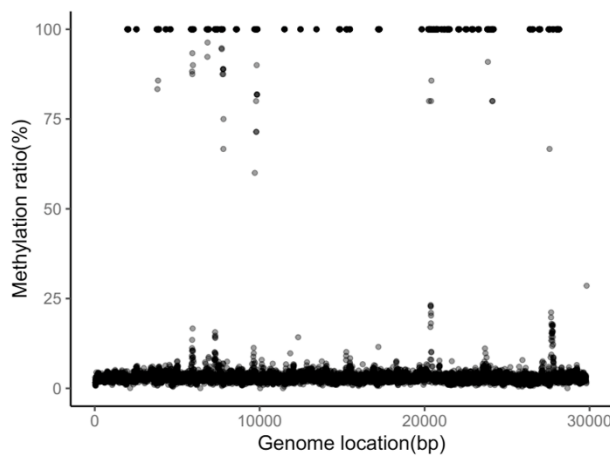
305

306 **Fig.S11 False-positive rate of ERCC (External RNA Controls Consortium)**
307 **RNA bisulfite sequencing.**

308 ERCC RNA was synthesized from RNA without m⁵C, subjected to bisulfite
309 treatment, and used for library construction. To further enhance the accuracy
310 of RNA-BSseq detection, we used the ERCC to test the false positive rate of
311 our method and to select a suitable cut-off (coverage > 5, methylation ratio >
312 95%, false positive ~ 0.006).

313

314

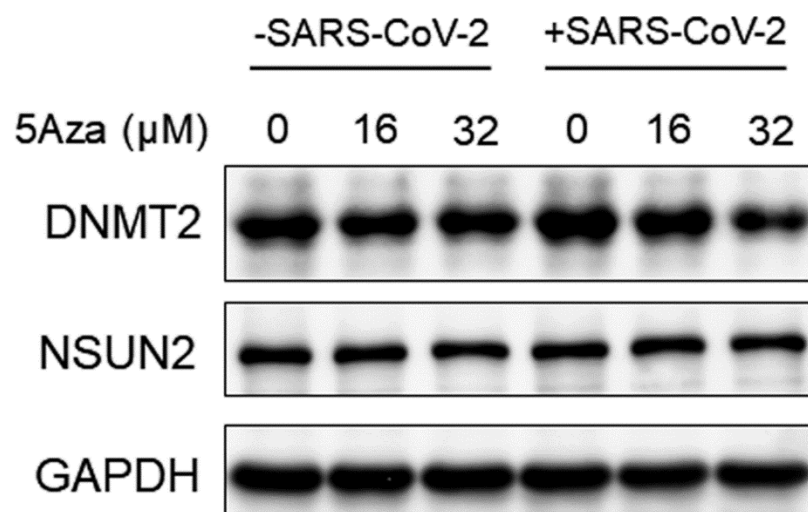


315

316 **Fig.S12 High confident m⁵C methylation sites on a delta variant of**
317 **SARS-CoV-2**

318 Vero E6 cells were infected with 1 moi delta variant of SARS-CoV-2. 24 hours
319 later, total RNA was extracted. m⁵C methylation sites were detected by RNA-
320 BSseq. There were five minimum methylation supporting reads per point. Data
321 are averaged from three technological repeats.

322



323

324 **Fig.S13 The effect of 5Aza treatment on the expression of DNMT2 and**
325 **NSUN2 protein.**

326 Mock or SARS-CoV-2 (moi=0.1) infected Vero E6 cells were treated with
327 indicated concentration of 5Aza. After 24 h, cells were lysed with RIPA buffer,
328 and the lysates were subjected to western blot for detecting indicated proteins.

329

330

331

332

333

334

335

336 **Supplementary Table 1**

337

338 **Table 1-1 The viral genome RNA mutant analysis comparison to SARS-**339 **CoV-2 reference genome after 5Aza treatment**

Genome Position	Reference Allele	Alternate Allele	GenoType	REFDepth	ALTDepth	Ref annotation Position	Protein.Position.Amino acids change
10	T	A	T/T	157	29	5'UTR	-
565	T	C	C/C	42	73716	gene-orf1ab	QHD43415.1:p.100S
565	T	G	T/T	42	60	gene-orf1ab	QHD43415.1:p.100S>R
7334	C	T	C/T	30312	47391	gene-orf1ab	QHD43415.1:p.2357H>Y
7334	C	G	C/C	30312	46	gene-orf1ab	QHD43415.1:p.2357H>D
7334	C	A	C/C	30312	6	gene-orf1ab	QHD43415.1:p.2357H>N
17321	C	T	C/T	19976	63384	ene-orf1ab	QHD43415.1:p.5686A>V
17321	C	G	C/C	19976	25	gene-orf1ab	QHD43415.1:p.5686A>G
17825	C	T	T/T	12	79423	gene-orf1ab	QHD43415.1:p.5854T>I
17825	C	A	C/C	12	12	gene-orf1ab	QHD43415.1:p.5854T>N
18844	G	A	G/A	18873	65715	gene-orf1ab	QHD43415.1:p.6194V>I
18844	G	C	G/G	18873	10	gene-orf1ab	QHD43415.1:p.6194V>L
21784	T	A	A/A	308	73557	gene-S	QHD43416.1:p.74N>K
21784	T	G	T/T	308	32	gene-S	QHD43416.1:p.74N>K
21784	T	C	T/T	308	24	gene-S	QHD43416.1:p.74N
23525	C	T	T/T	848	78868	gene-S	QHD43416.1:p.655H>Y
23525	C	A	C/C	848	11	ene-S	QHD43416.1:p.655H>N
23606	C	T	C/T	19736	59756	gene-S	QHD43416.1:p.682R>W
23606	C	G	C/C	19736	24	gene-S	QHD43416.1:p.682R>G
23606	C	A	C/C	19736	6	gene-S	QHD43416.1:p.682R
29573	G	A	A/A	19	73657	gene-ORF10	QHI42199.1:p.6V>I
29573	G	T	G/G	19	6	gene-ORF10	QHI42199.1:p.6V>F

340

341

342

343

344

345

346

347

348

349

350

351

352

353

354

355

356 **Table 1-2 The viral genome RNA mutant analysis comparison to SARS-**
 357 **CoV-2 reference genome after saline treatment (Control)**

Genome Position	Reference Allele	Alternate Allele	GenoType	REFDepth	ALTDepth	Ref annotation Position	Protein.Position.Amino acids change
18	T	G	T/T	1980	166	5'UTR	-
565	T	C	C/C	49	76463	gene-orf1ab	QHD43415.1:p.100S
565	T	G	T/T	49	11	gene-orf1ab	QHD43415.1:p.100S>R
7334	C	T	C/T	35181	48436	gene-orf1ab	QHD43415.1:p.2357H>Y
7334	C	G	C/C	35181	15	gene-orf1ab	QHD43415.1:p.2357H>D
17321	C	T	C/T	22730	62149	gene-orf1ab	QHD43415.1:p.5686A>V
17825	C	T	T/T	10	82113	gene-orf1ab	QHD43415.1:p.5854T>I
17825	C	A	C/C	10	25	gene-orf1ab	QHD43415.1:p.5854T>N
18844	G	A	G/A	21743	66770	gene-orf1ab	QHD43415.1:p.6194V>I
18844	G	C	G/G	21743	18	gene-orf1ab	QHD43415.1:p.6194V>L
18844	G	T	G/G	21743	6	gene-orf1ab	QHD43415.1:p.6194V>L
21784	T	A	A/A	340	80300	gene-S	QHD43416.1:p.74N>K
21784	T	C	T/T	340	24	gene-S	QHD43416.1:p.74N
21784	T	G	T/T	340	24	gene-S	QHD43416.1:p.74N>K
23525	C	T	T/T	995	82974	gene-S	QHD43416.1:p.655H>Y
23525	C	A	C/C	995	10	gene-S	QHD43416.1:p.655H>N
23606	C	T	C/T	22874	61149	gene-S	QHD43416.1:p.682R>W
23606	C	A	C/C	22874	5	gene-S	QHD43416.1:p.682R
29573	G	A	A/A	22	81434	gene-ORF10	QHI42199.1:p.6V>I

358

359

360

361

362